

- Modular orthopaedic devices are a feature of total joint replacements today
- Benefits:
 - Allow surgeons to choose from a variety of available implant sizes, designs & material options for the procedure & patient specific requirements
- Drawbacks:
 - Can lead to fretting fatigue & corrosion, due to the resulting micro-motion & contact stresses
 - Found at mismatched surfaces during cyclical loading, resulting in interface wear
 - Can lead to implant rejection, due to wear debris induced osteolysis

Example Modular Implants

METS Modular
Total Femur
(Stanmore Implants, UK)



- Components
 - Acetabular Cups (Liners & Shells)
 - Femur Stems
 - Femur Heads
 - Knee
 - Total System (Knee, Femur, Head & Cup)

- Materials

- Cobalt Chromium Alloys
- Technical Ceramics
- Titanium Alloys
- Steel Alloys
- Polymers (UHMWPE & PEEK)



Trinity™ Cup &
MiniHip™ Stem
(Corin, UK)

OVERVIEW & AIM

Overview

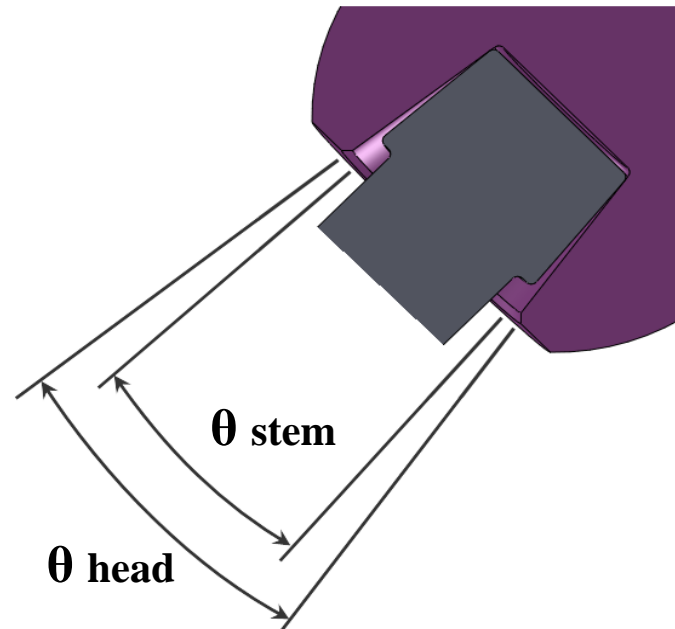
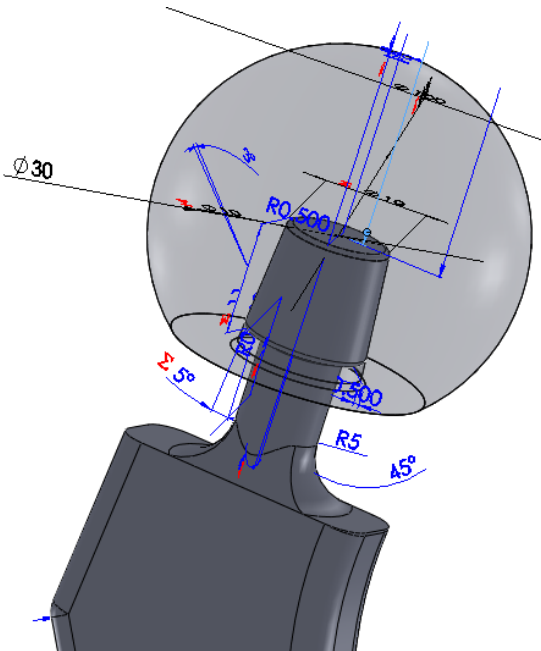
Assessment of Femur Head & Stem

→ Variation in interface design

1. Tolerances
2. Geometric parameters
3. Materials

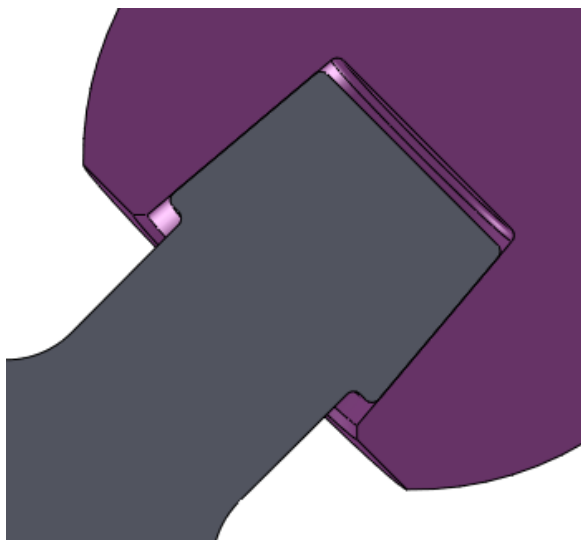
→ Study look at variation in interface angle (θ):

1. θ_{stem}
2. θ_{head}



- Quantify & compare fretting fatigue for three specific fits between the femur stem & head

- θ stem = θ head
- θ stem > θ head
- θ stem < θ head



Ideal fit

θ stem = θ head



Positive mismatch

θ stem > θ head

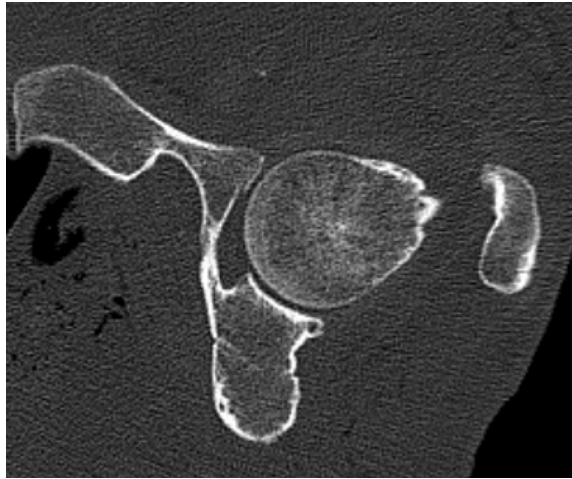


Negative mismatch

θ stem < θ head

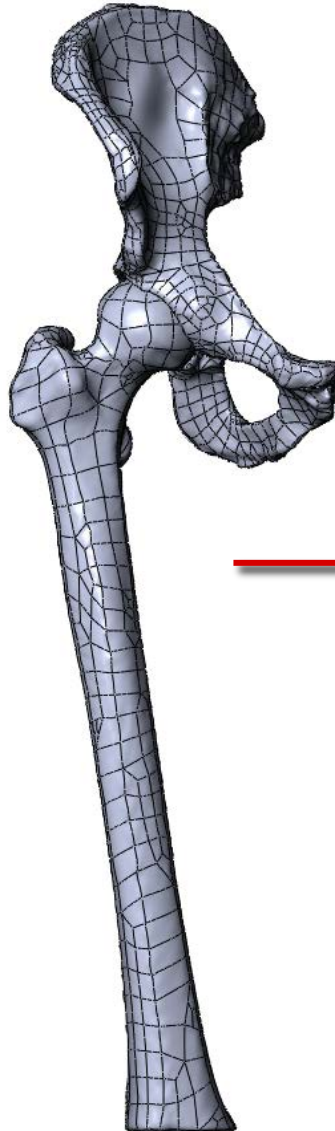
GEOMETRY GENERATION, MATERIALS & LOADS

Geometry Generation from CT Scans

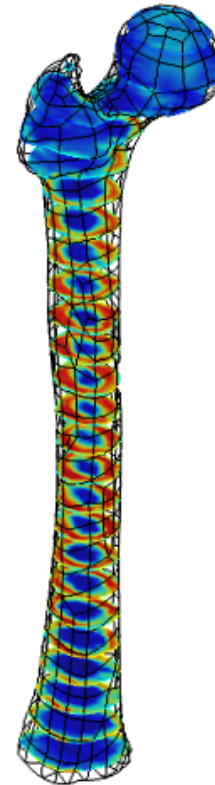


CT scan
(Patient Specific)

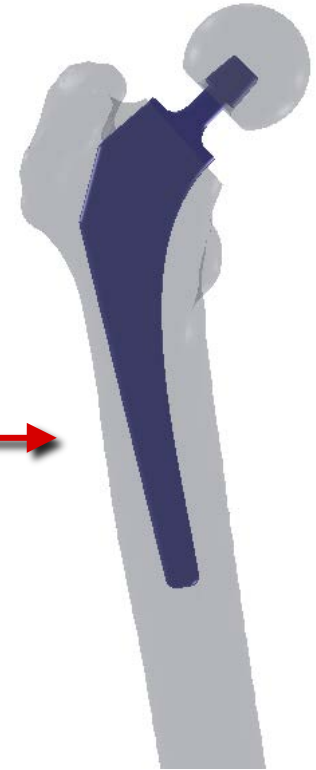
Geometry
Generation



Bone Property
Mappings
(Density)



Implant Femur
Stem & Head
Design



Bone Properties (Density, Modulus & nu Relationships)

Density

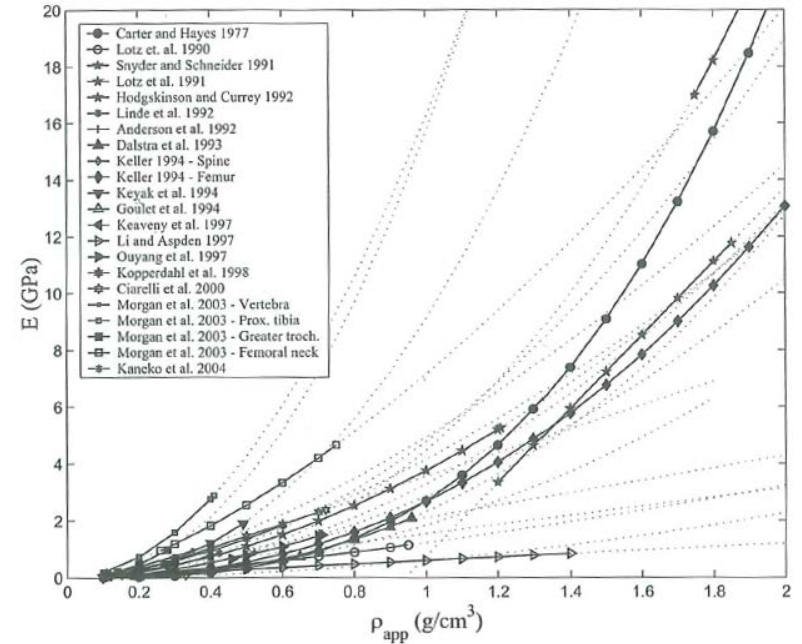
$$\rho = f(HU)$$

Young's Modulus

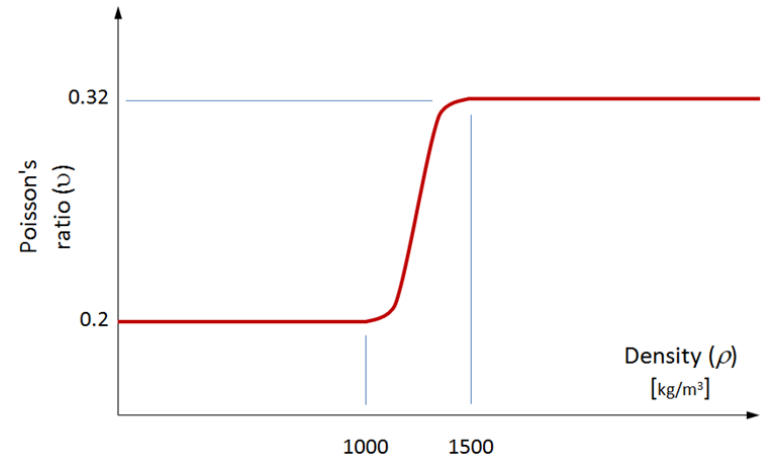
$$E = 6.4\rho_{app}^{1.54}$$

Poisson's Ratio

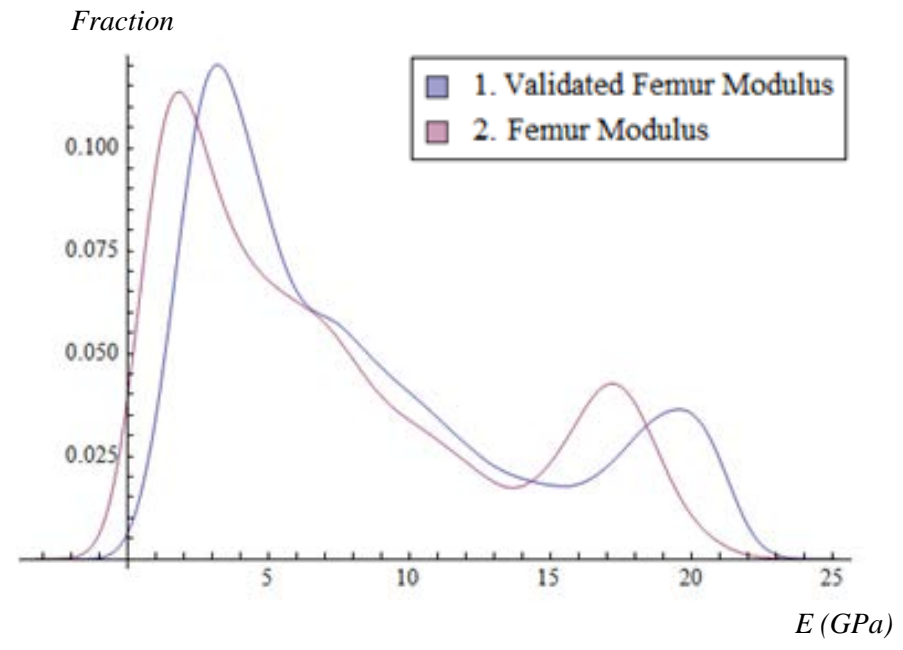
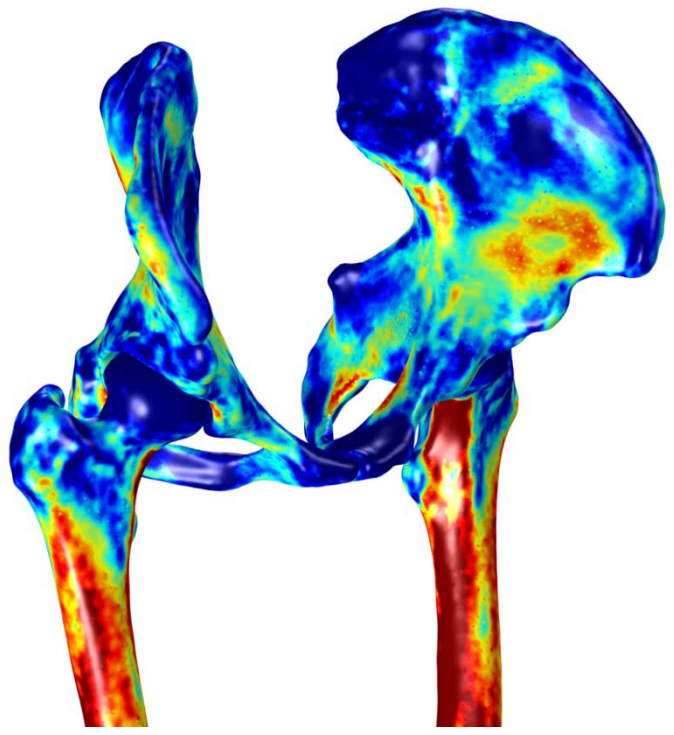
$$\nu = \begin{cases} 0.2 & \text{if } \rho < 1000 \\ \frac{0.12}{500}\rho_{app} - 0.04 & \text{if } 1000 \leq \rho \leq 1500 \\ 0.32 & \text{if } \rho > 1500 \end{cases}$$



Helgason [2008]



Material Properties (Validation: Patient Specific)

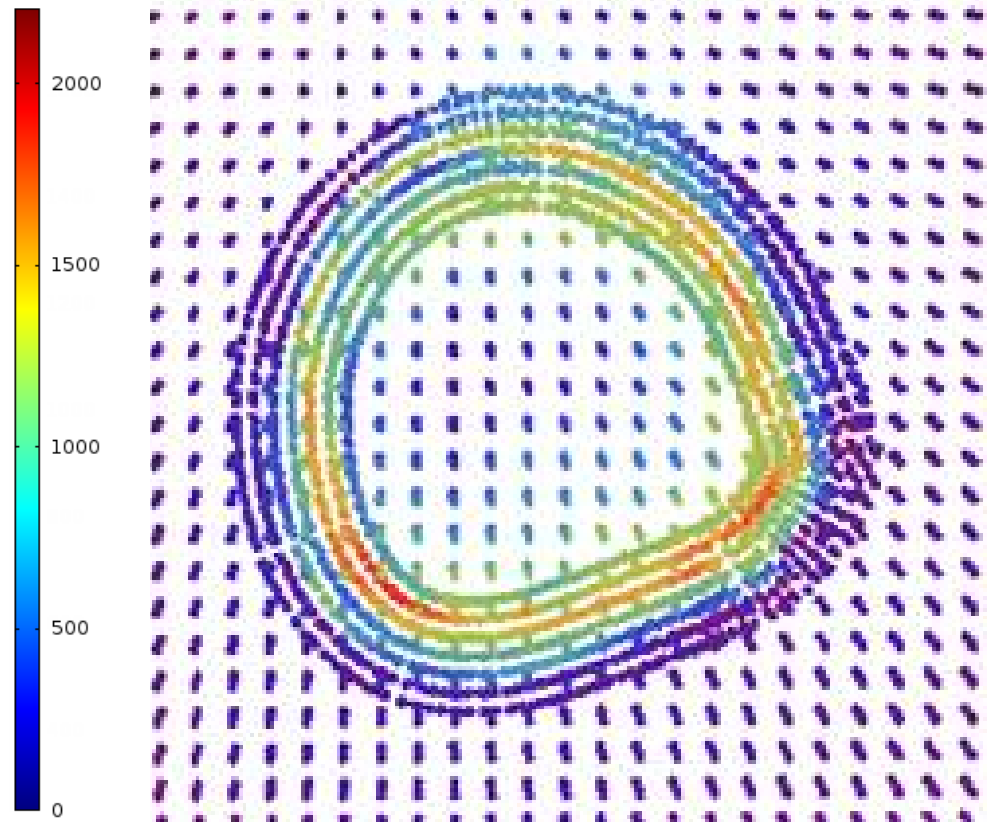


Femur	Minimum	Mean	Maximum
Model	0.1	8.3	23.3
Validated Femur [Helgason 2008]	0.5	6.6	22.5

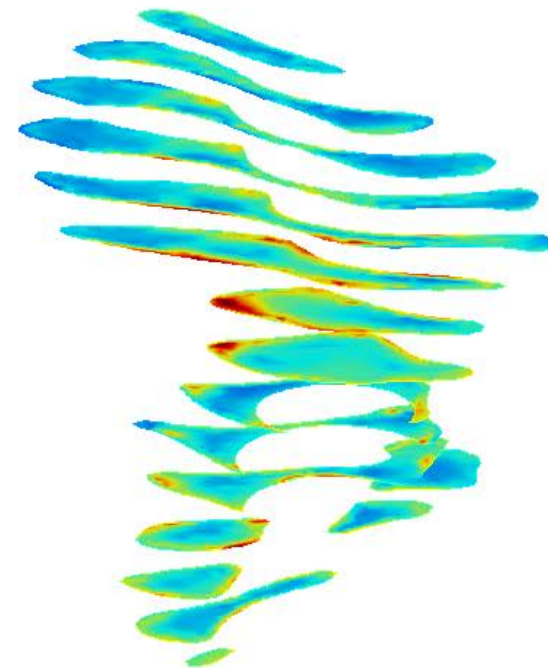
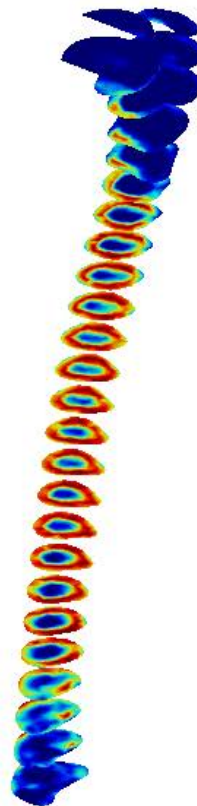
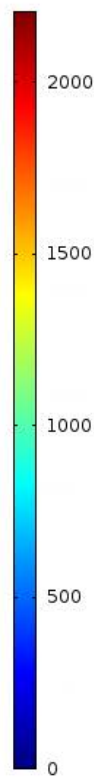
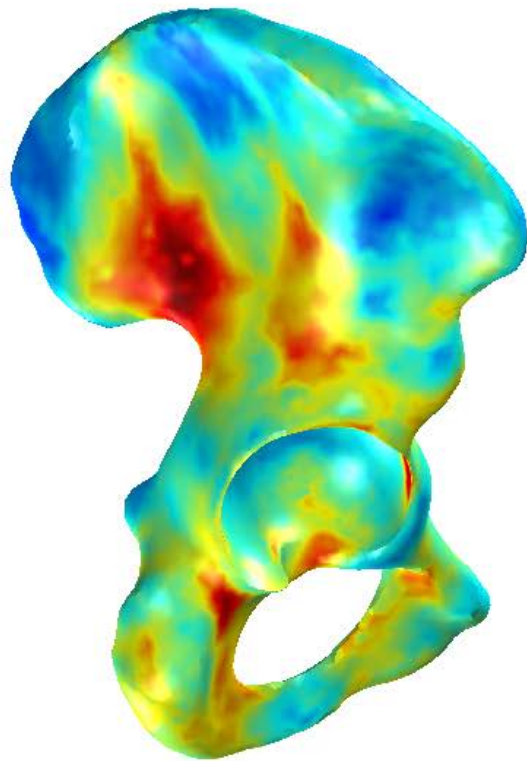
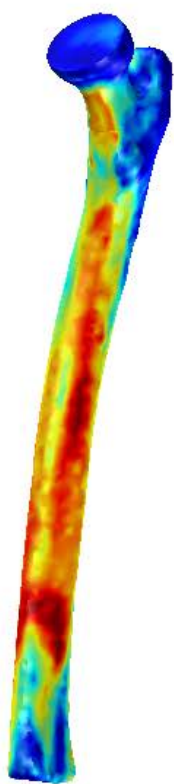
Density Refinement (Femur Cortical Surface)

Bone density mapping was refined around cortical surface to capture high variation in density which may be missed out by using standard grid method

Density Point Cloud Illustrating
Grid vs. Refined Cortical
Surface



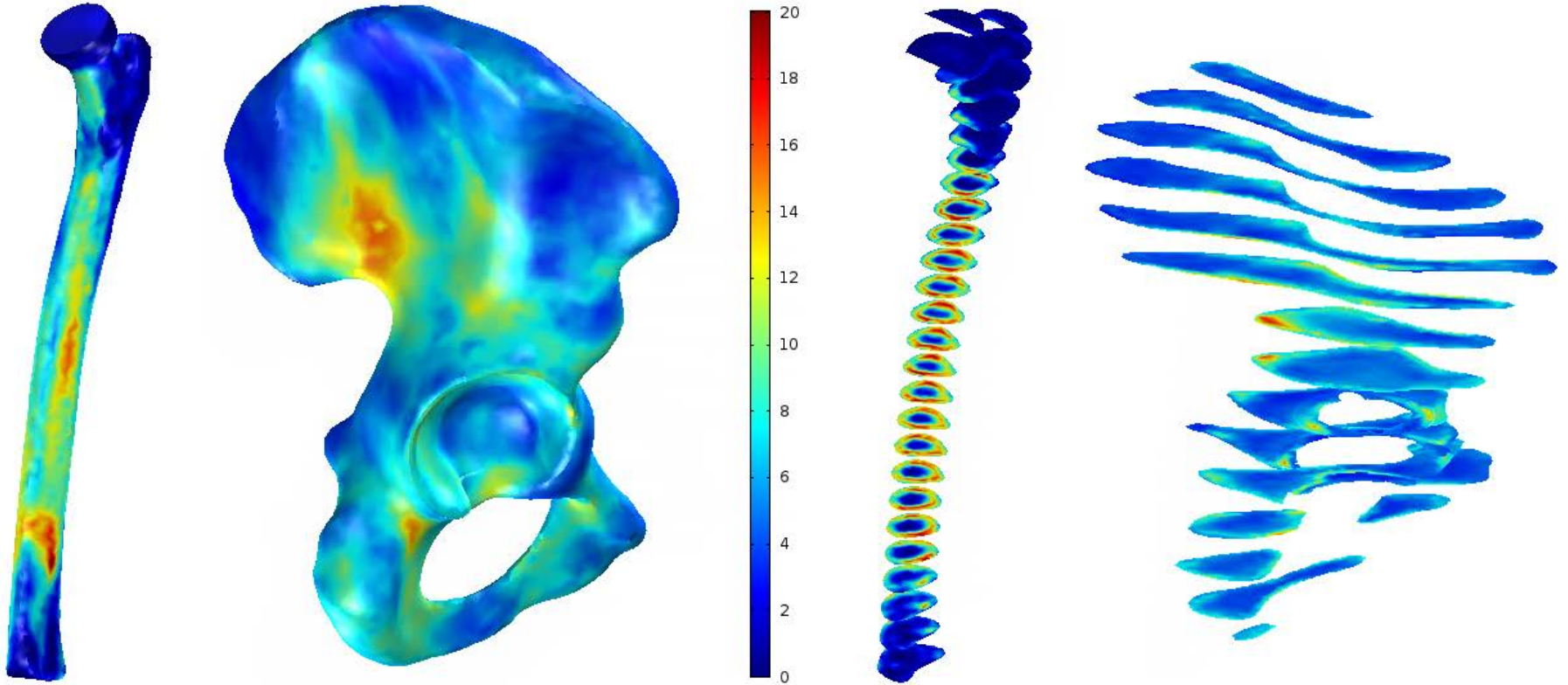
Density (kg/m³)



Surface Plot

Sectional Slice Plot

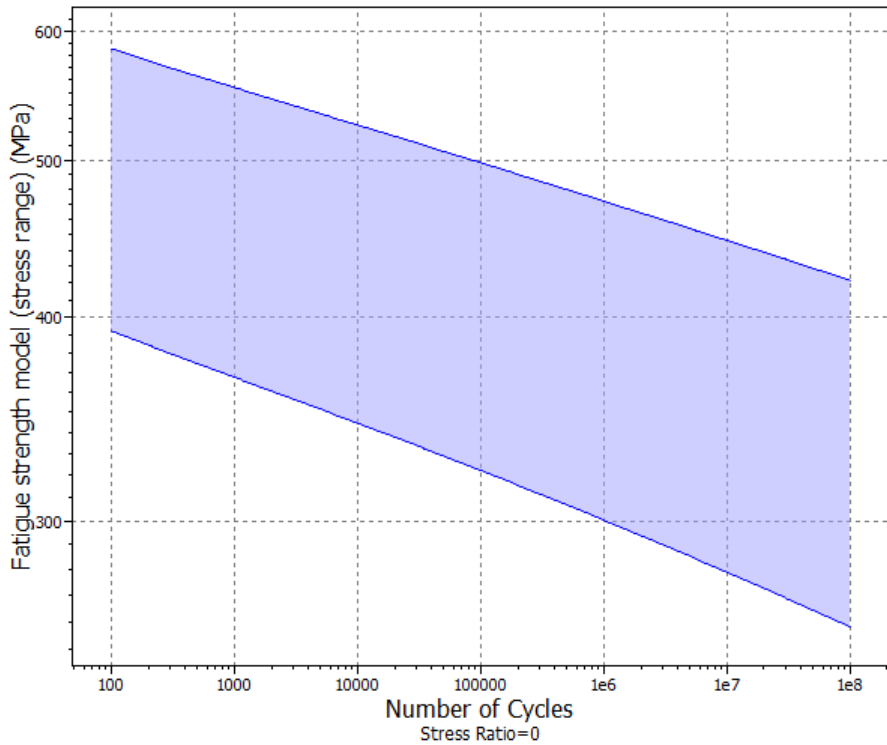
Young's Modulus (GPa)



Surface Plot

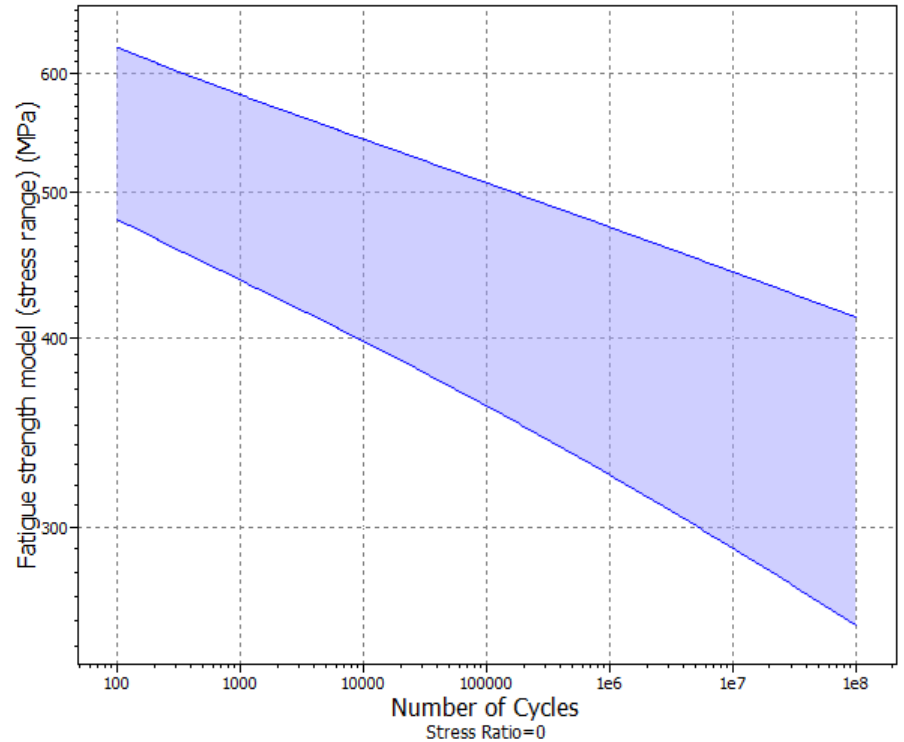
Sectional Slice Plot

Implant Materials (SN Curves & Fatigue Properties)



Ti-6Al-4V

Stem



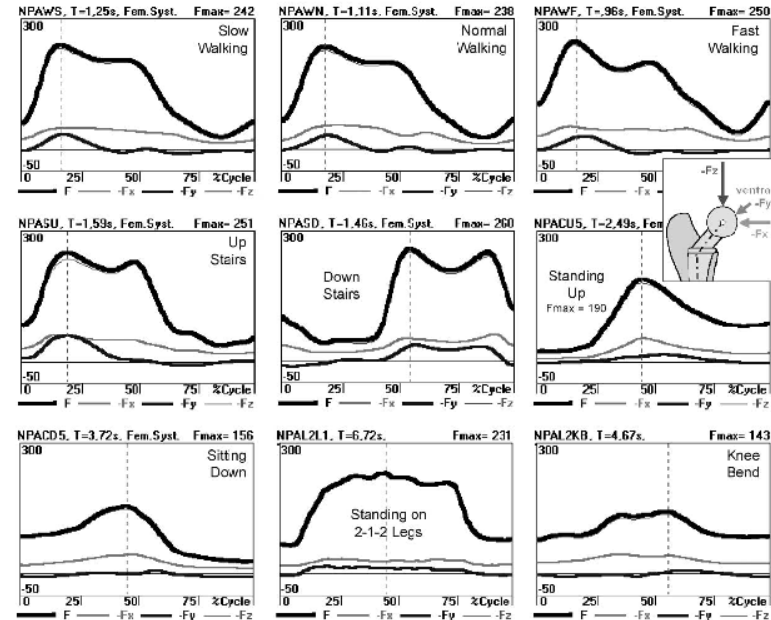
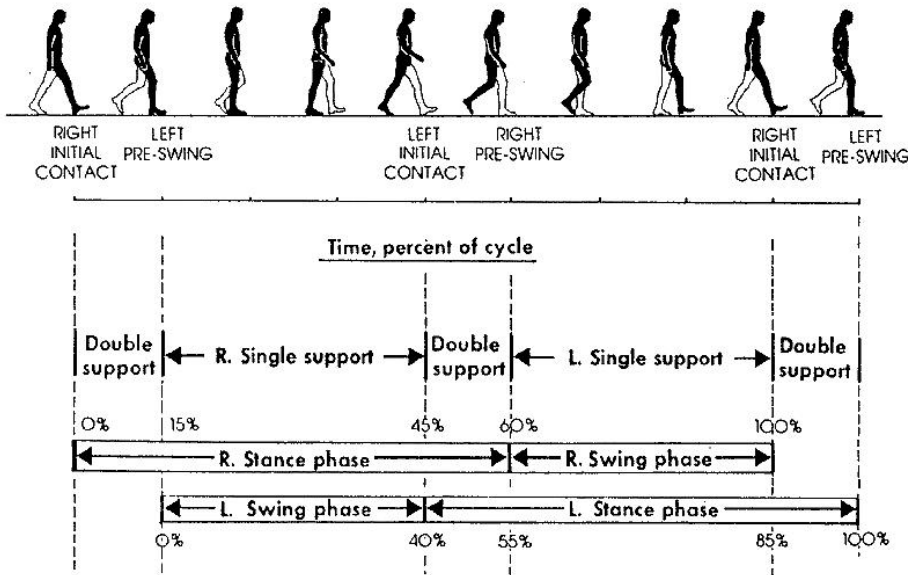
Nickel-Co-Cr

Head

FE Model Load Validation

- Kinematic load data obtained from Bergmann et al.[6], based on average physical data from 4 patient data sets
- Loads muscle force boundary conditions to FEA model

Cyclic loading applied on femur head & abductor muscle

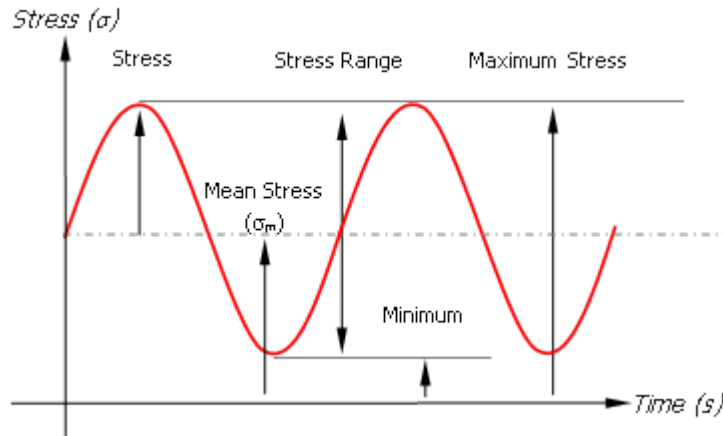


Kinematic model data for different activities (typical patient) [6]

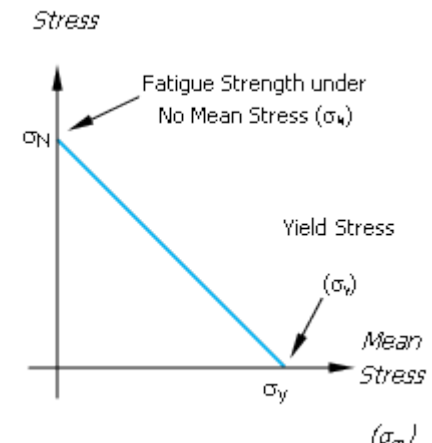
THEORY

General Material Fatigue

- General Material fatigue described by relating:
 - Oscillating mean stress & stress amplitude
- Using either the Goodman, Gerber or Soderberg relationships, an equivalent stress amplitude with no mean stress can then be found from the mean stress & stress amplitude
 - Soderberg's relationship is utilised as conservative compared to Goodman or Gerber relationships.
- This equivalent stress amplitude with no mean stress, can then be read off physical SN curves ($R=-1$) to obtain the predicted number of cycles to failure for the fatigued part due to cyclic loading.



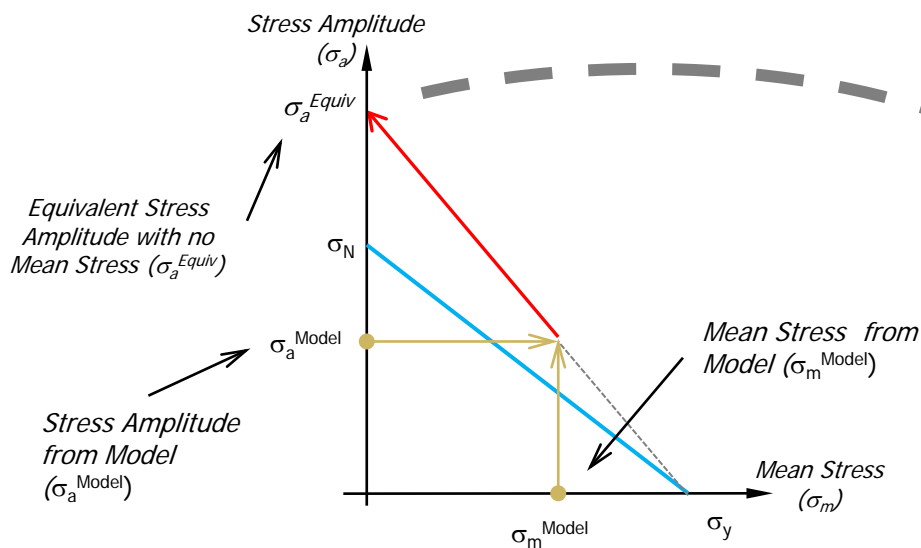
a) Combined Cyclic & Mean Stress Schematic



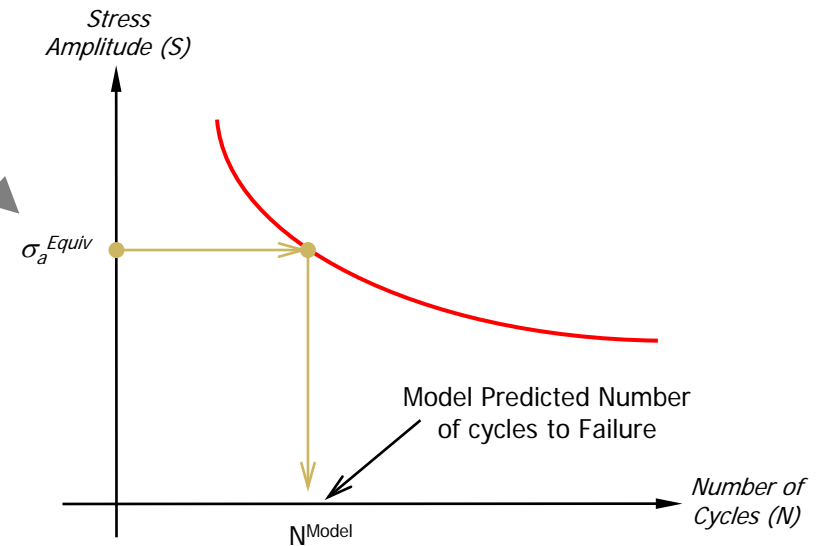
b) Soderberg's Amplitude & Mean Stress Relationship

Equivalent $\sigma_{\text{amplitude}}$ & Cycles to Failure

- For each material domain, mean stresses & stress amplitudes are calculated over single walking gait load cycle.
- Using Goodman diagram & Soderberg relationship
 - Equivalent stress amplitude with zero mean stress are obtained
 - Stress Ratio (R) = -1
- Equivalent stress amplitudes are then read off SN curves (function) to predict number of cycles to failure for the fatigued part due to cyclic loading.



a) Obtaining Equivalent Stress Amplitude with no Mean Stress from Soderberg's Amplitude & Mean Stress Relationship



b) Predicted of Number of Cycles to Failure from SN Curves using Equivalent Stress Amplitude with no Mean Stress

Fretting Fatigue Theory (SN Curve Adjustment)

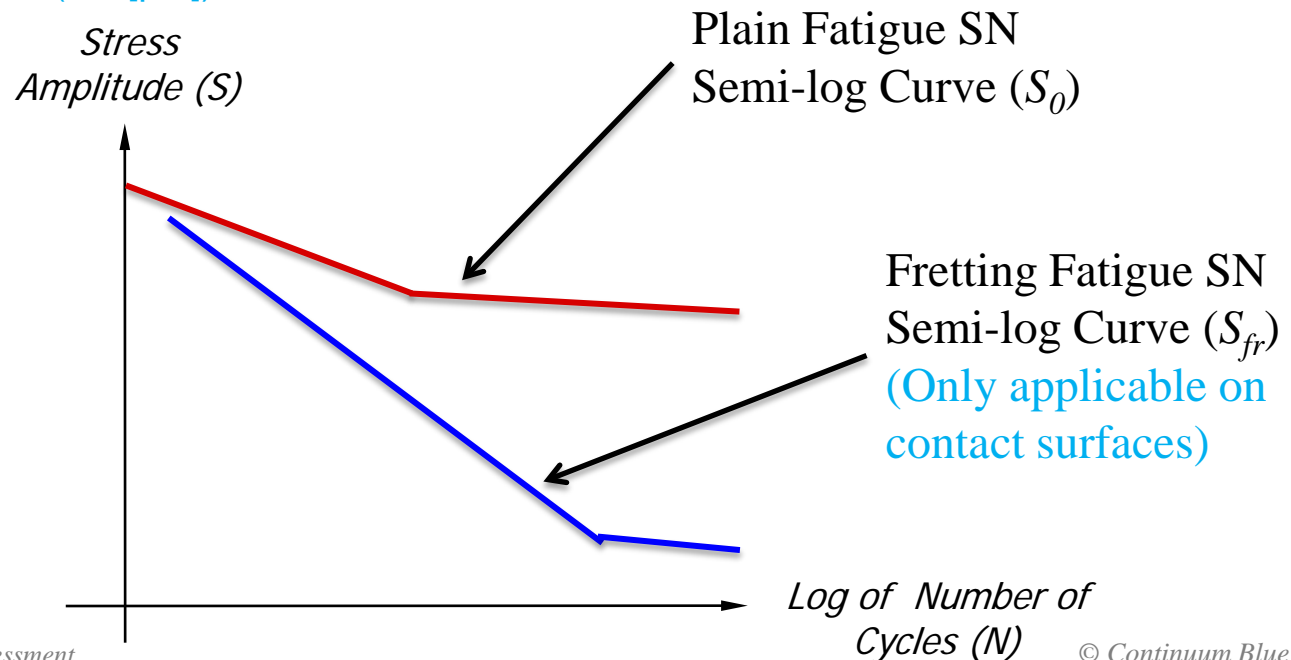
For Fretting Fatigue, the SN curves were adjusted by the following equation for fretting strength (S_{fr}) to take account of early prediction to failure due to fretting:

$$S_{fr} = S_o - 2 \times \mu \times p_o \times [1 - e^{-l/k}]$$

Where,

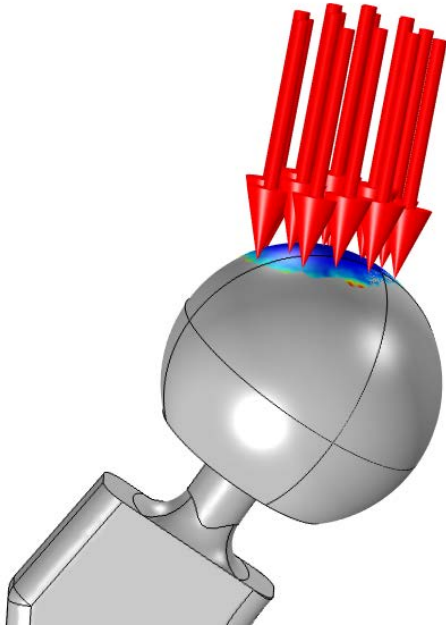
- S_{fr} = Fretting fatigue strength [MPa]
- S_o = Fatigue strength in the absence of fretting [MPa]
- μ = Coefficient of friction
- p_o = Contact pressure [MPa]
- l = Fretting amplitude [μm]
- k = Constant (3.8 [μm])

Relation between Plain Fatigue vs. Fretting Fatigue

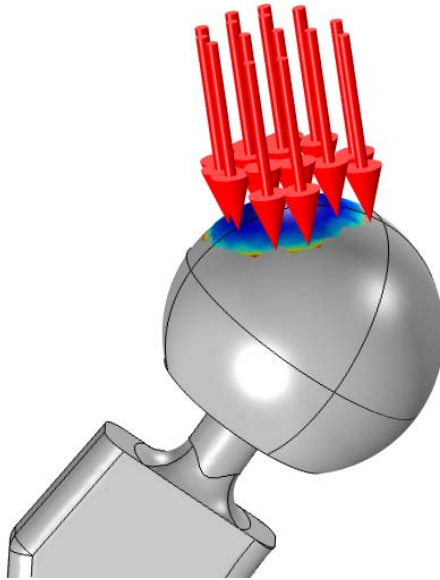


RESULTS

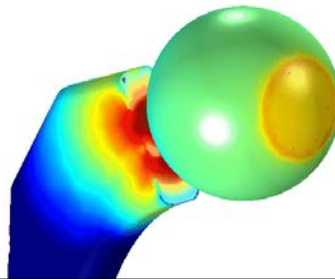
Implant Stress & Load (Walking Gait Cycle)



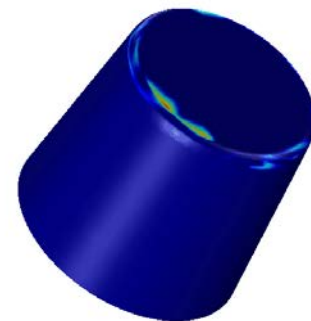
Load at 20% gait cycle



Load at 60% gait cycle

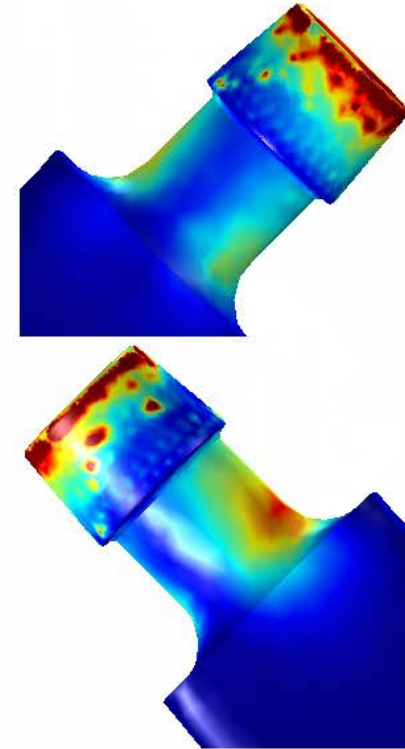
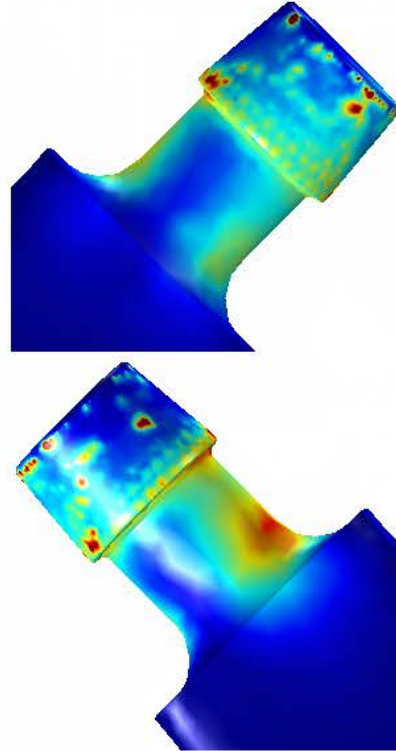
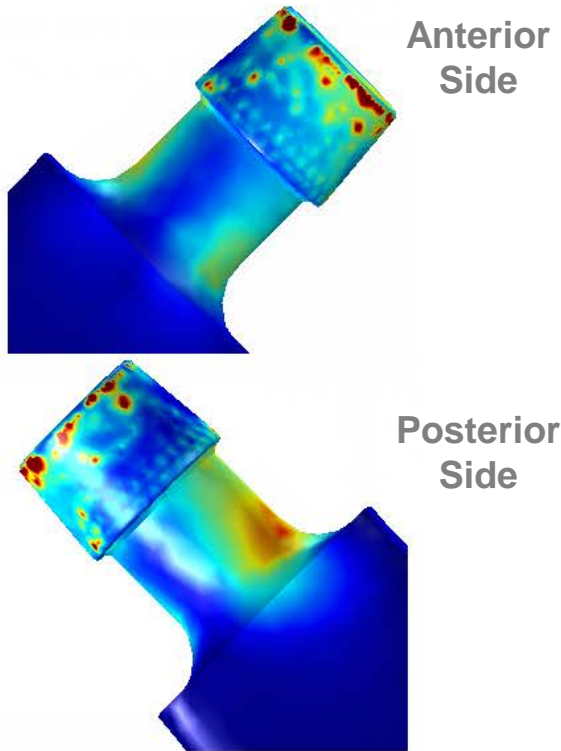


Load vectors during gait cycle



von Mises stress on the stem

Results: von Mises Stress



Ideal fit

$$\theta_{\text{stem}} = \theta_{\text{head}}$$

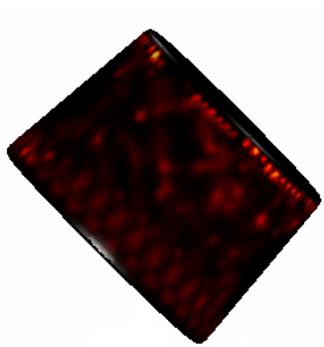
Positive mismatch

$$\theta_{\text{stem}} > \theta_{\text{head}}$$

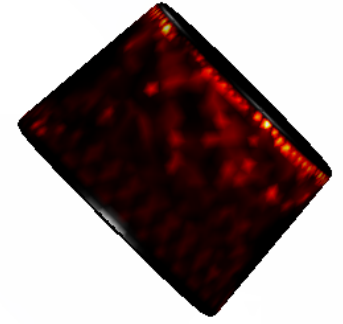
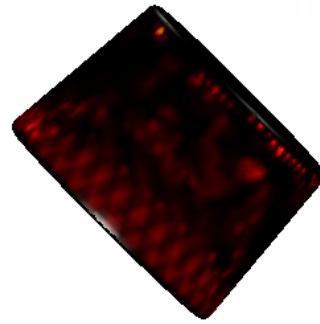
Negative mismatch

$$\theta_{\text{stem}} < \theta_{\text{head}}$$

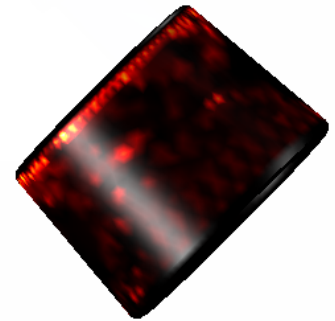
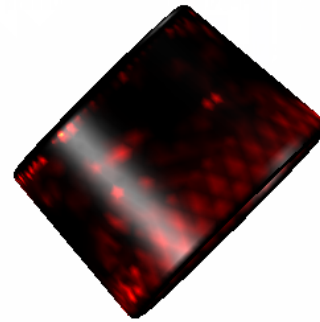
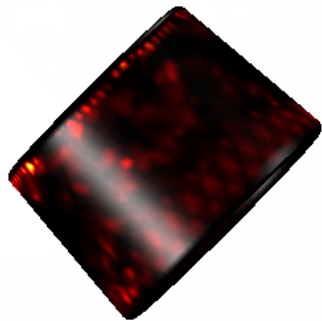
Results: Contact Pressure



Anterior
Side



Posterior
Side



Ideal fit

$$\theta \text{ stem} = \theta \text{ head}$$

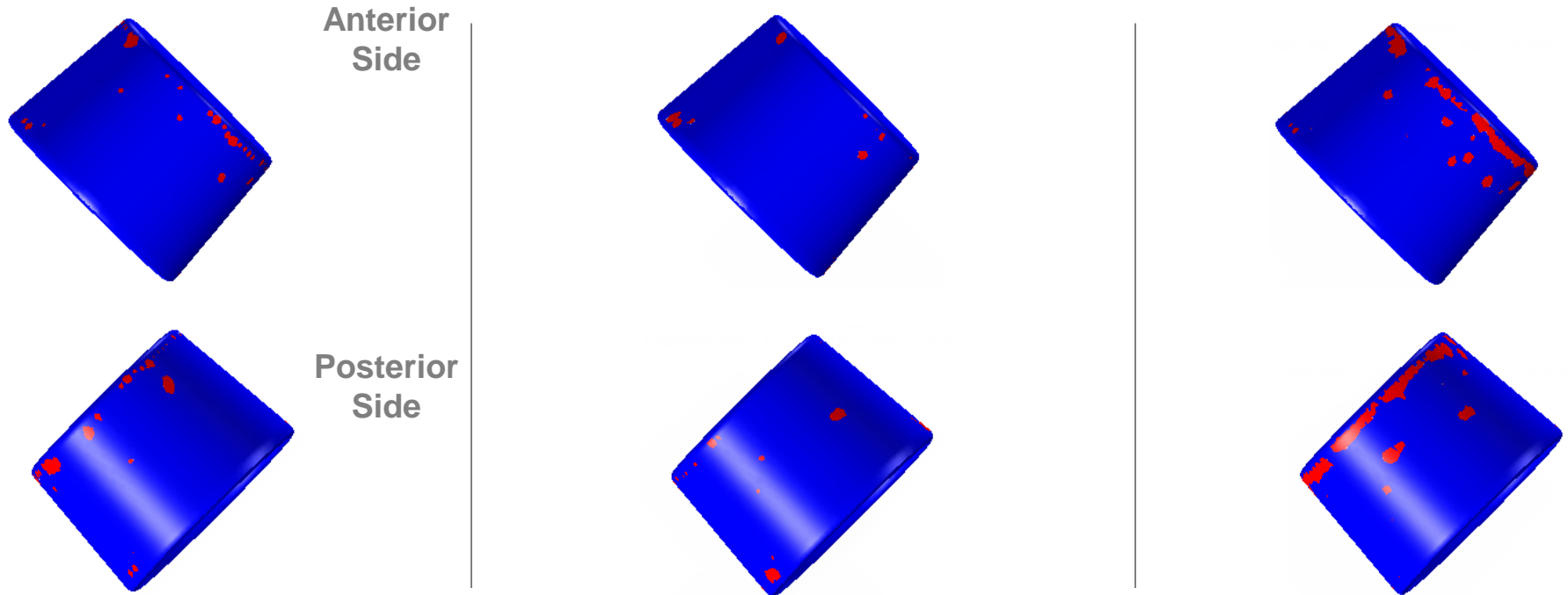
Positive mismatch

$$\theta \text{ stem} > \theta \text{ head}$$

Negative mismatch

$$\theta \text{ stem} < \theta \text{ head}$$

Results: Areas of Fretting Fatigue



Area of evident fretting fatigue (% of total contact area):

Ideal fit

0.29%

Positive mismatch

0.13%

Negative mismatch

1.01%

- Under walking load (gait cycle) conditions for particular modular implant configuration:
 - The 'ideal fit' is not actually the best design to minimise fretting fatigue as would have been thought
 - Negative misalignments give rise to larger observed fretting fatigue
- A slight positive misalignment minimises fretting fatigue, for this particular modular implant configuration

- Only 3 variations in stem misalignment assessed
 - No sensitivity analysis was performed on magnitude of misalignment

- Only assessed one a particular modular implant configuration & design
 - Additional design & or geometric parameters may play a larger role in determining magnitude of fretting fatigue

- Only assessed two specific materials, CoCr (head) against Titanium Alloy (Stem)
 - The results may change with material change
 - Softer head vs. harder stem
 - Harder stem vs. softer head

Conclusion

- A Fretting fatigue model has been implemented in COMSOL
- Validation of fretting fatigue models vs. physical tests is on going
- More work needs to be done to fully describe the fretting fatigue characteristics of misaligned implants, in terms of
 - Misalignment sensitivity
 - Material variation (Soft on hard vs. hard on soft)
 - Additional designs & or geometric characteristics
 - Surface finishes, roughness & coatings may change results

- Keller et al, Young's modulus, bending strength, and tissue physical properties of human compact bone, J Orthop Res, 8(4):592-603, 1990
- Helgason, Subject specific finite element analysis of bone with particular application in direct skeletal attachment of a femoral prosthesis, PhD Thesis, University of Iceland, 2008.
- Carter & Hayes. The compressive behaviour of bone as a two phase porous structure, Journal of Bone and Joint Surgery (AM), 59(7):954-962,1977.
- Gray et al, Experimental validation of a finite element model of a human cadaveric tibia, J Biomech Eng. 130(3), 2008
- Stülpner, M.A. et al, A three-dimensional finite analysis of adaptive remodelling in the proximal femur. Journal of Biomechanics, 10:1063-1066, 1997
- Scannell & Prendergast, Cortical and interfacial bone changes around a non-cemented hip implant: Simulations using a combined strain/damage remodelling algorithm. Medical Engineering & Physics, 31:477-488, 2009
- Turner et al, Computational bone remodelling simulations and comparisons with DEXA results. Journal of Orthopaedic research, 23:705-712, 2005.
- Heller et al, Musculo-skeletal loading conditions at the hip during walking & stair climbing, J Biomech, 2001
- Heller et al, Determination of muscle loading at the hip joint for use in pre-clinical testing, J Biomech, 2005
- Abdullah, K., Study of factors affecting taper joint failures in modular hip implant using finite element modelling, 2010
- Grupp et al, Modular titanium alloy neck adapter failures in hip replacement - failure mode analysis and influence of implant material, 2010
- Kumar et al, Evaluation of fretting corrosion behaviour of CP-Ti for orthopaedic implant applications, 2010
- Shigley, J.E., Mechanical Engineering Design: First Metric Edition, McGraw-Hill, 1986
- Hearn, E.J., Mechanics of Materials 2, Butterworth-Heinemann, 1997
- Stachowiak & Batchelor, Engineering Tribology, Elsevier Butterworth-Heinemann, 2005
- Gwidon W. Stachowiak, Andrew W. Batchelor, Engineering Tribology 3RD Edition pp. 635-636

THANK YOU!

Contact: *Dr Mark Yeoman*

E: mark@continuum-blue.com

M: +44 (0) 7916 283 970

T: +44 (0) 1342 824 921

W: www.continuum-blue.com